Organic & Biomolecular Chemistry

Accepted Manuscript

ROYAL SOCIETY OF CHEMISTRY

www.rsc.org/obc

Synthesis and Evaluation of Photoresponsive Quencher for Fluorescent Hybridization Probes

Marina Kovaliov[a], Chaim Wachtel[b], Eylon Yavin[c],

and Bilha Fischer[a]

[a]Department of Chemistry, Bar-Ilan University, Ramat-Gan 52900, Israel

[b]The Mina and Everard Goodman Faculty of Life Sciences, Bar-Ilan University, Ramat-Gan 52900, Israel

[c]School of Pharmacy, Institute for Drug Research, The Hebrew University of Jerusalem, Ein Karem, Jerusalem 91120, Israel

Address correspondence to:

Bilha Fischer

Department of Chemistry, Bar-Ilan University, Ramat-Gan 52900, Israel

Fax: 972-3-6354907

Tel.: 972-3-5318303

e-mail: bilha.fischer@biu.ac.il

ABSTRACT

Nowadays, most nucleic acid detection using fluorescent probes relies on quenching of fluorescence by energy transfer from one fluorophore to another or to a nonfluorescent molecule (quencher). The most widely used quencher in fluorescent probes is 4-((4-(dimethylamino)phenyl)azo)benzoic acid (DABCYL). We targeted a nucleoside-DABCYL analogue which could be incorporated anywhere in an oligonucleotide sequence and in any number, and used as a quencher in different hybridization sensitive probes. Specifically, we introduced 5-(4-((dimethylamino)phenyl)azo)benzene)-2'-deoxy-uridine (dU^{DAB}) quencher. The photoisomerization and dU^{DAB}'s ability to quench fluorescein emission have been investigated. We incorporated dU^{DAB} in to a series of oligonucleotide (ON) probes including strand displacement probes, labeled with both fluorescein (FAM) and dU^{DAB}, and TaqMan probes bearing one or two dU^{DAB} and a FAM fluorophore. We used these probes for the detection of a DNA target in real-time PCR (RT-PCR). All probes showed amplification of targeted DNA. dU^{DAB} modified TaqMan RT-PCR probe was more efficient as compared to a DABCYL bearing probe (93% vs. 87%, respectively). Furthermore, dU^{DAB} had a stabilizing effect on the duplex, causing an increase in T_m up to 11 ºC. In addition we showed the photoisomerisation of the azobenzene moiety of dU^{DAB} and the dU^{DAB} triply-labeled oligonucleotide upon irradiation. These findings suggest that dU^{DAB} modified probes are promising probes for gene quantification in real-time PCR detection and as photoswitchable devices.

INTRODUCTION

Fluorescent methods are widely used to detect nucleic acids sequences in homogeneous solution genetic assays. The design, synthesis, and biological evaluation of modified nucleotides and oligonucleotides have attracted substantial interest in recent years.[1-8] Applications of those analogues include homogeneous DNA sequencing techniques[9] for molecular diagnostics as basis of personalized medicine,[10, 11] single nucleotide polymorphism (SNP),[12-17] as well as for identification and quantification of nucleic acids.[18-21] Fluorescence and fluorescence quenching form the basis of the majority of detection systems, such as specific displacement hybridization probes,[22-24] Molecular Beacons (MBs),[25] Scorpion,[9] and TaqMan probes.[6]

TaqMan is a widely used probe for the detection of amplicon specific PCR products by homogenous fluorescence detection in real-time. The probe is a ss-oligonucleotide, containing one fluorescence dye at the 5' end and one quencher at the 3' end. The probe is complementary to sequence located within the amplicon and binds to the amplicon during the annealing step of the PCR reaction. Upon elongation the DNA polymerase will come in contact with the probe, and the 5'→3' exonuclease activity of the polymerase will degrade the probe, releasing the fluorophore from the quencher and thus increasing the fluorescence intensity.[26, 27] The fluorescent signal is thus dependent on the amplification of the specific amplicon and increases with the increase in the amount of DNA after each cycle of PCR.

An alternative fluorescence probe system for the detection and quantification of nucleic acids is a specific displacement hybridization probe.[5, 22, 28] This probe contains a pair of complementary singly labeled oligonucleotides consisting of the probe strand with a fluorophore label and a short, quencher-labeled complementary oligonucleotide strand.

When annealed to each other there is no fluorescent signal, since the fluorophore and quencher are in close proximity. However, during the PCR cycle and upon amplification of the target, the two oligomers can anneal to the target instead of each other, generating a fluorescent signal. These probes can be used for different homogeneous DNA or RNA detection techniques, such as standard real time PCR (RT-PCR).[9]

Properly designed probes should have low background fluorescence. Increasing the quenching efficiency would necessary result in an increased signal to background ratio. An approach that can lead to reduced background fluorescence is achieved by moving a quencher or dye from a terminal position to an internal position of an oligonucleotide. A decreased distance between the quencher and the fluorescent dyes causes a more efficient Förster resonance quenching,[29] and diminishes the original probe fluorescence. This method was used in PCR TaqMan probes, for several dye-quencher pairs e.g., FAM-TAMRA[30] and FAM-BHQ1.[31] Another strategy to increase the quenching efficiency consists of adding several quencher molecules. Recently MBs have been synthesized using a FAM (fluorescein) reporter and two or three DABCYL (4-((4-(dimethylamino)phenyl)azo)benzoic acid) quenchers at 3'-end of the probe. This strategy results in an enhancement of quenching efficiency from 92.9% to 99.7%.[32]

DABCYL is characterized by an absorption maximum at 475 nm and has a quenching range from 400-550 nm, yet, has an extremely low fluorescence quantum yield.[33, 34] This property has allowed its use to quench a wide range of common fluorescent dyes such as FAM (λ_{em} 520 nm), TET (λ_{em} 535 nm), JOE (λ_{em} 548 nm), and HEX (λ_{em} 550 nm). The quenching ability of DABCYL was intensively investigated in numerous biological systems with oligonucleotides for nucleic acid detection or peptides for monitoring enzymatic activity.[35] Generally DABCYL is incorporated into an oligonucleotide as a

phosphoramidite monomer or by labeling a nucleoside via a long backbone-amide-type,[36] or aliphatic linker.[37, 38]

In addition to its use as a quencher in oligonucleotide probes, azobenzene derivatives are highly studied photochromic compounds because they undergo *cis-trans* photoisomerisation, which can be switched at particular wavelengths of light.[39-41] The photoinduced isomerisation of azobenzene moieties has been applied to the switching functions of various biomolecules.[42-47] Recently simple azobenzene units were incorporated into short oligonucleotides within the strands using prochiral diol[48] or *D*- or *L*-threoninol based spacers,[49, 50] which were used to gain reversible formation and dissociation of DNA duplex or triplex by photoregulated *cis-trans* isomerisation of the azobenzene.[51] Although these azobenzene containing oligonucleotides demonstrated significant photosensitivity, the above mentioned modifications alter the oligonucleotide backbone structure as they lack both the deoxyribose unit and the nucleic acid base.[52] Furthermore, some of these azobenzene dyes absorb strongly only in the UV region, thus reducing their ability to be used as a quencher in biomolecular systems.[53, 54]

Many technologies to control hybridization of oligonucleotides have been developed, and the most common approach is via inclusion of an azobenzene group as part of a short oligonucleotide.[55] Photo-control of the DNA duplex formation can be used as a robust tool for elucidating and controlling DNA involving biological processes.[56] The control of the formation and dissociation of DNA duplex in photoisomerization of azobenzene can lead to direction of protein–DNA interactions for example; photo-control of enzyme activity,[50, 57] photocontrol of transcription by RNA polymerase and photoregulation of DNA transcription.[58, 59] In addition these DNA photoregulated duplexes can be used as photoresponsive DNA nanomechanical molecular devices which opens and closes by UV-light.[49]

In view of azobenzene biological significance, the aim of the present work has been to develop a novel photoswitchable quencher, to be incorporated in any number and anywhere in fluorescent oligonucleotide hybridization probes, and to be used for the detection of nucleic acids sequence. Since DABCYL is a common quencher used for labeling fluorescent probes, we aimed to develop a nucleoside bearing DABCYL moiety with a minimal modification of the former's structure.

For this purpose we designed and synthesized 5-[4-(dimethylamino)azobenzene]-2'-deoxyuridine (dU^{DAB}), **1**, related to the structure of DABCYL, **2** (Fig. 1).[60] In addition, we studied the photophysical properties and quenching efficiency of this photoresponsive nucleoside. Furthermore, we describe the incorporation of **1**, into oligonucleotide strand displacement and TaqMan based probes containing one, two or three dU^{DAB} quenchers for the detection of a DNA target sequence. Finally, we demonstrated the duplex stability of these probes and used them in real time qPCR.

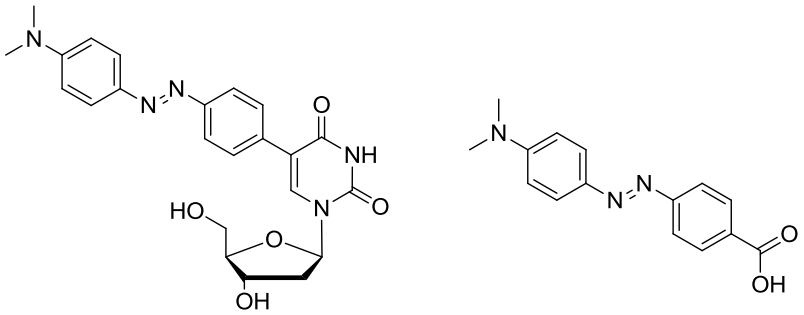

Figure 1. The structure of 5-(4-((dimethylamino)phenyl)azo)benzene)-uridine (dU^{DAB}), **1**, and the known quencher DABCYL, **2**.

RESULTS AND DISCUSSION

Design of dU^{DAB} - a quencher for fluorescent hybridization probes

We targeted the synthesis of a modified uridine analogue, bearing a 4-((dimethylamino)phenyl)azo)benzene- moiety at C5-position, dU^{DAB}, as a potential quencher for fluorescent hybridization probes. dU^{DAB} potentially may have several important advantages over existing DABCYL quenchers.[37, 38] Firstly, the possibility to attach the modified uridine at any position of the designed oligomer, could allow the incorporation of more than one modified nucleoside. Secondly, the structure of dU^{DAB} should not perturb double helix formation and therefore not greatly alter the stability of the formed duplex. Finally, the presence of an azobenzene moiety that can undergo configurational change upon excitation with light at a certain wavelength may lead to its use in photoregulation of a duplex composed of a dU^{DAB} containing oligomer and the complementary nucleic acid sequence.

Synthesis of dU^{DAB}-phosphoramidite

Dabcyl-modified uracil, dU^{DAB}, was designed to have a 4-(dimethylamino)azobenzene moiety at C5 which does not interfere with hydrogen bonding sites of uracil and therefore retains the base pairing ability with adenine. Our synthetic strategy was first to prepare 4,4-(dimethylamino)azobenzene boronic ester **5**, and then to conjugate it to C5' protected uridine **6**, by Suzuki palladium-catalyzed cross-coupling reaction. Compound **5** was synthesized in a one-pot reaction, containing 4-(4,4,5,5-tetramethyl-1,3,2-dioxaborolan-2-yl)aniline **3**, and *N*,*N*-dimethylaniline. In the first step, the diazonium ion of the aniline boronic ester derivative, **4** was generated with sodium nitrite in HCl.[61] Diazonium ion **4**, reacted with dimethylaniline to give **5** in 21% yield (Scheme 1). Boronic acid pinacol ester, **5**, was then coupled to 5'-DMT-5-I-dU **6**, under Suzuki conditions[62] using TPPTS, Na_2CO_3 and $Pd(OAc)_2$ in CH_3CN:H_2O (2:1), to obtain

derivative **7** as a orange solid in 85% yield. Compound **1**, was obtained in 90% yield upon treatment of **7** with 3% trichloroacetic acid in dichloromethane (Scheme 2).

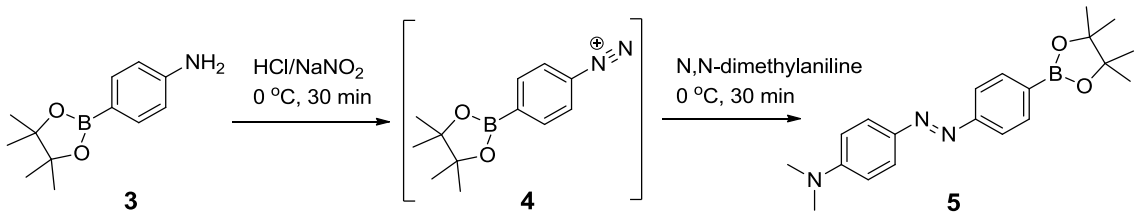

Scheme 1 Synthesis of boronic pinacol ester reagent, compound **5**.

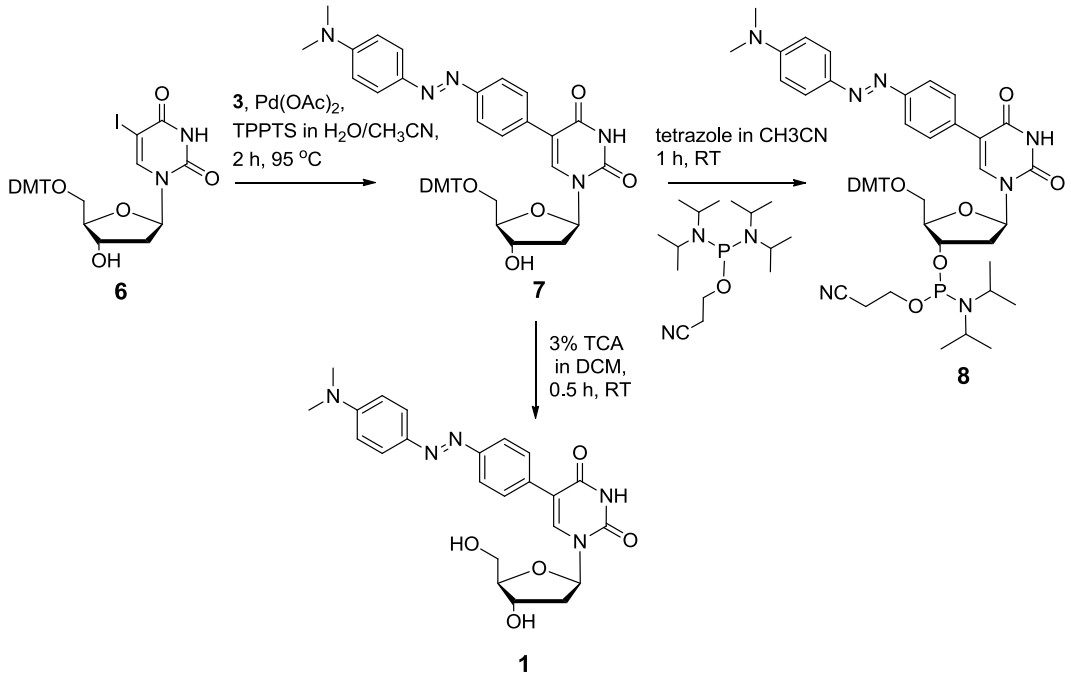

Scheme 2 Synthesis of dU^{DAB} phosphoramidite **8**.

Compound **7** was treated with 2-cyanoethyl *N,N,N',N'*-tetra-isopropylphosphoramidite in presence of tetrazole. A concentrated solution of dU^{DAB} phosphoramidite monomer, **8** was obtained after filtration of the diisopropylammonium tetrazolide, and was diluted with CH_3CN to a formal concentration of 0.1 M and immediately used for automated synthesis of oligonucleotides. ^{31}P NMR spectrum of **8** showed two typical phosphoramidite signals at 149 ppm, for two diastereoisomers. Monomer **8** allowed the

facile incorporation of dU^{DAB} into oligonucleotides at any internal or terminal position *via* a conventional oligonucleotide synthesis.

X-ray crystallographic analysis of 1

2'-Deoxynucleoside analogue **1** was crystallized from DCM and hexane by slow evaporation. X-Ray analysis of the crystal structure revealed that the nucleoside analogue is a very good structural mimic of thymidine (Fig. 2).

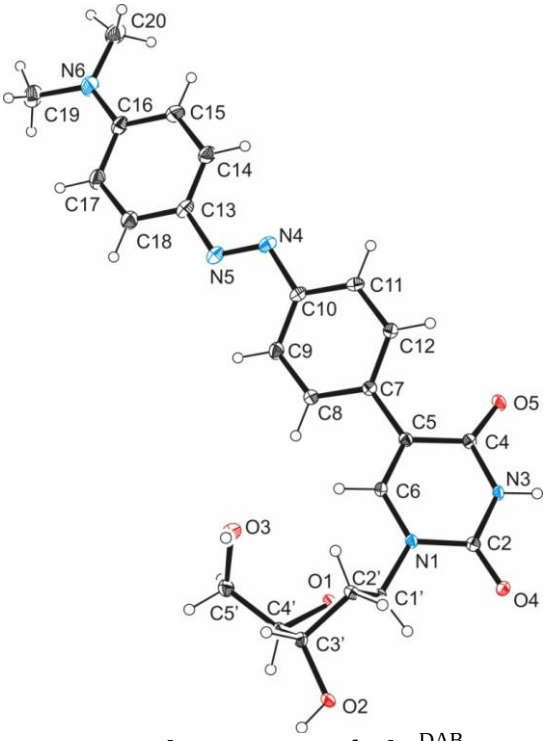

Figure 2 X-ray crystal structure of dU^{DAB}, **1**, showing its azobenzene chromophore in its *trans* configuration**.**

The compound has an *anti* conformation around the glycosidic bond and *S*-type (C2'-*endo*) pucker in the sugar moiety. The structure also reveals that azobenzene is in its expected *trans* configuration with the angle between both aromatic rings flanking the azo-bond measured as 10.8 °, and a torsional angle of 32.7 ° between the uracil ring and the C5- aromatic ring. A comparison of average bond lengths and bond angles of **1** vs. published structural data for thimidine are given in Table S5, Supporting Information.[63, 64]

Absorption spectra and photoisomerisation study of 1, dU^{DAB}

To assess the photochromic behavior of dU^{DAB} we monitored the changes that occurred upon irradiation at 365 nm in DCM (Fig. 3A). Absorption spectrum of *trans* isomer is characterized by a large absorption band around 420 nm attributed to strong ππ* transition which overlap with a small band around 549 nm attributed to weak nπ* transition.[42] By irradiating with UV-light at 365 nm, a time-dependent decrease in the intensity of the absorption band was observed due to *trans*-to-*cis* isomerization (Fig. 3B), while the reverse *cis*-to-*trans* isomerization was achieved via thermal relaxation in the dark (Fig. 3C).

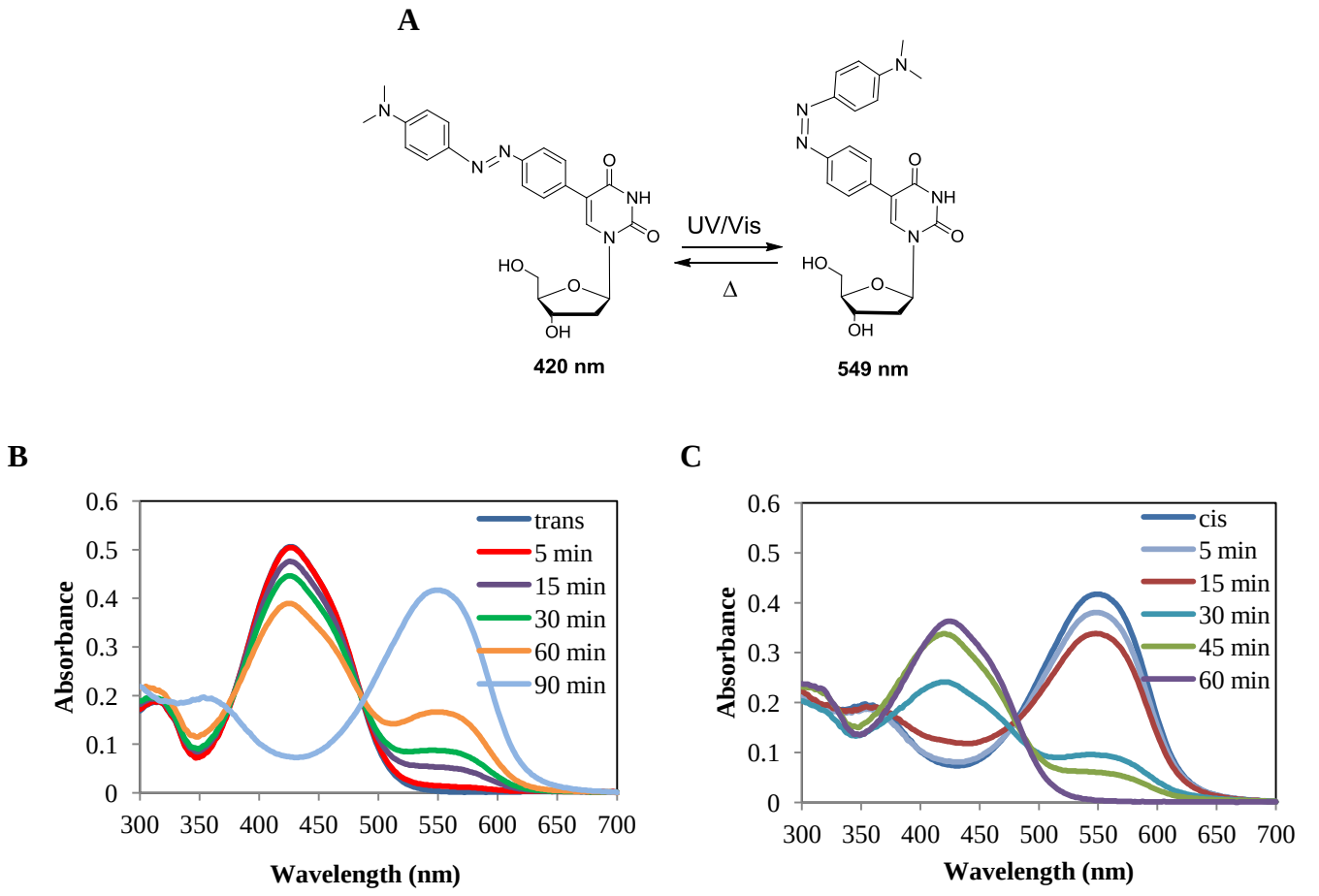

Figure 3 (A**)** Schematic representation of reversible *trans-cis* photoisomerization of the photochromic nucleoside dU^{DAB}, **1**. (B) Absorption spectra of 15 µM dU^{DAB}, **1**, in dichloromethane undergoing *trans-cis* photoisomerization upon irradiation with UV-light at 365 nm. (C**)** Absorption spectra of 15 µM dU^{DAB}, **1,** in dichloromethane undergoing *cis-trans* photoisomerization upon thermal relaxation in the dark.

This irradiation–dependent structural change was also confirmed by ^{1}H NMR in deuterated acetone (Fig. S11 and Fig. S12, Supporting Information). The solution was irradiated several times and the original spectrum was recovered each time in the dark, which indicates that the reaction is completely reversible.

Design and synthesis of dU^{DAB}-labeled oligonucleotide RT-PCR probes

In order to evaluate the quenching efficiency of dU^{DAB} nucleoside, we designed and synthesized three types of fluorescent hybridization sensitive probes for homogeneous detection of DNA. These probes hybridized to a target sequence derived from the human β-actin gene.

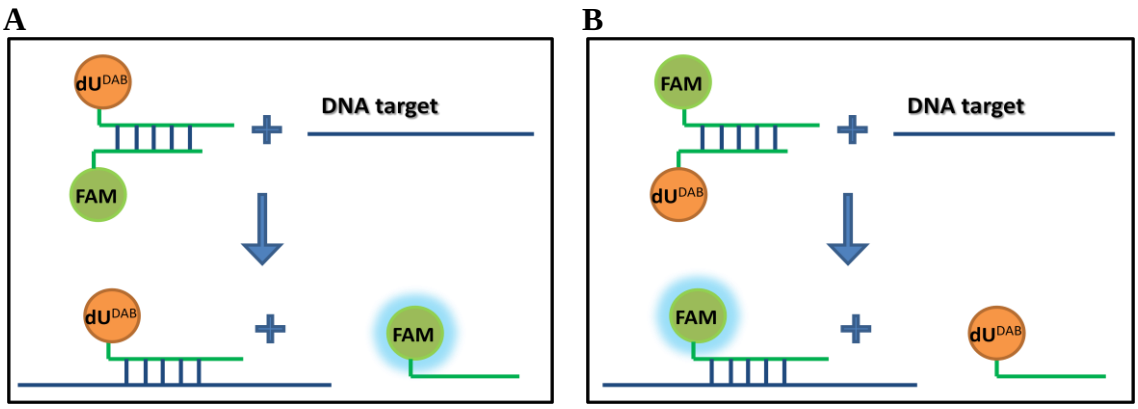

Figure 4 Schematic drawings of a dU^{DAB} double-stranded probe and the working principle. The double stranded probes are composed of two complementary oligonucleotides of different length. (A) The long strand bears a quencher dU^{DAB} and the short bears a fluorophore, FAM. In the presence of the DNA target, the fluorophore bearing strand is displaced and becomes fluorescent. **(**B) The long strand bears a fluorophore, FAM and the short bears a quencher, dU^{DAB}. In the presence of the DNA target, the quencher, dU^{DAB} bearing strand is displaced and the duplex becomes fluorescent.

Figure 4 illustrates the design and working process of the probes based on displacement hybridization. We designed two types of strand displacement probes, where the dU^{DAB} is at the 5'-end of the long strand or at the 3'-of the short strand. General design rules for displacement probes have been previously published.[22] The length difference between the two strands of the probe should be a minimum of 3 base pairs. The quencher strand

should not compete with the fluorescent, reporting strand, but should hybridize to unbound excess of it, preventing background signal. Hence, first we labeled the 5'-end of the long (19-mer) strand, with dU^{DAB} and the 3'-end of the short (15-mer) strand was coupled with FAM. When not bound to a target, the duplex probe is not fluorescent, due to close proximity of the fluorophore and the quencher. In the presence of the DNA target, the strands separate, the dU^{DAB}-labeled long strand is base paired to the target, and the short FAM labeled strand becomes free and fluorescent (Fig. 4A). We based this type of dU^{DAB} –labeled displacement probe on a 2'-OMe-RNA scaffold, since such oligonucleotides are not substrates for RNaseH and show resistance to degradation by RNA- or DNA-specific nucleases.[65] In addition to being stable to standard handling and nuclease resistance, 2'-OMe-RNA oligomers form more stable hybrids with complementary DNA strands than equivalent RNA and DNA sequences.[66, 67] This kind of probe could be used for the detection of DNA/RNA in homogeneous solutions.

The second type of ds-probes included a 3'-end FAM labeled long strand and a short strand labeled with dU^{DAB} at 5'-end (Fig. 4B). In the end of the process the long strand labeled with FAM binds to the DNA targetand becomes fluorescent. Quenching is completely dependent on the physical proximity of the fluorophore and the quencher.[68] Therefore, to enhance quenching efficiency we designed the same probe with three dU^{DAB} quenchers. These displacement probes could be used for the detection of nucleic acids in homogeneous hybridization in solution and in RT-PCR analysis.

In addition we designed a third type of RT-PCR probes containing one or two dU^{DAB} quenchers based on classic TaqMan probes. In the TaqMan method, fluorescence quenching occurs by FRET within the intact probe. During the extention phase of PCR, the probe binds to its specific target and is degraded by the 5'→3' exonuclease activity of Taq polymerase. This releases the quencher and fluorophore into solution, where they

are spatially separated, resulting in an increase in fluorescent signal. Here, we suggested that incorporation of more than one dU^{DAB} quencher could improve performance of the probe by increasing the signal to noise ratio.

Table 2 Oligonucleotides used in this study[a]

Oligonucleotide	Sequence 5'→3'
ON1-2'-OMe	dU^{DAB}AUGACGAGUCCGGCCCCU-PO_3^{-2}
ON2	GCCGGACTCGTCATA-FAM
ON3	FAM-ATGACGAGTCCGGCCCCT-PO_3^{2}
ON4	GCCGGACTCGTCAdU^{DAB} -PO_3^{2}
ON3	FAM-ATGACGAGTCCGGCCCCT-PO_3^{2}
ON5	dU^{DAB} GCCGGACdU^{DAB} CGTCAdU^{DAB} -PO_3^{2}
ON6	FAM-TATGACGAGTCCGGCCCCdU^{DAB} -PO_3^{2}
ON7	FAM-TAdU^{DAB} GACGAGTCCGGCCCCdU^{DAB} –PO_3^{2}
ON8-target	GACGATGGAGGGGCCGGACTCGTCATACTCCTGCT
ON9-primer Forward	TGGATCAGCAAGCAG
ON10-primer Reverse	GCATTTGCGGTGGAC
ON11	FAM-TATGACGAGTCCGGCCCCT-DABCYL
ON12-scrambled	TGCTCCTGGTGAACAAGCTCAAGTGGAACCTGGCC

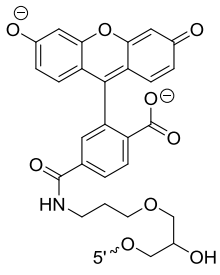

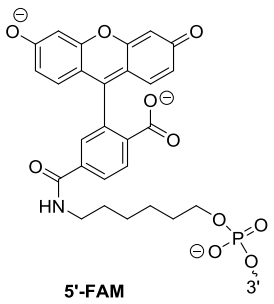

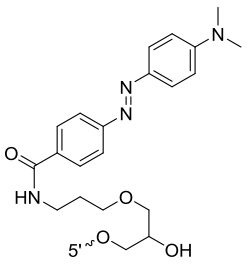

[a]For each oligonucleotide used in this study, the nucleic acid sequence is given, written in the 5'→3' direction. There are four types of oligonucleotides: three pairs of ONs for strand displacement probes, labeled with FAM and dU^{DAB}, TaqMan probes, PCR primers and the complementary ONs as DNA target.

To prepare strand-displacement and TaqMan dU^{DAB}-labeled probes, that target the β-actin gene sequence, we synthesized a series of oligonucleotides **ON1-ON11** (Table 2). For this purpose, we used dU^{DAB} phosphoramidite **8**, and commercially available carboxyfluorescein (FAM) phosphoramidite.

Specifically, we prepared three pairs of ONs, for double strand displacement probes and TaqMan probes, labeled with FAM and dU^{DAB}, PCR primers and the complementary and scrambled ONs as DNA targets. We annealed the oligonucleotides to prepare the following strand displacement dU^{DAB} labeled probes; **ON1:ON2** probe with dU^{DAB} at the 5'-end of the long strand 19-mer, **ON1**, which hybridizes to the DNA target, and FAM at the 3'-end of the short 15-mer strand, **ON2**. **ON3:ON4** probe with FAM at the 5'-end of the long 18-mer, strand **ON3**, which hybridizes to the DNA target, and dU^{DAB} at the 3'-end of the short 14-mer strand, **ON4**. And finally **ON3:ON5** probe, where the short strand was labeled with three dU^{DAB} quenchers. To prepare one or two dU^{DAB} labeled TaqMan based probes, we synthesized **ON6** and **ON7**. We used 19-nucleotide-long probes targeting the β-actin gene sequence, and two primers **ON9** and **ON10**. Finally, we compared **ON6** and **ON7** to TaqMan labeled with commercial quencher DABCYL, **ON11**. In addition, we used **ON12**-scrambled target in order to establish the specificity of the strand displacement probe.

Absorption and Photoisomerisation of ON5

dU^{DAB} absorbs visible light and undergoes *cis-trans* isomerisation (Fig. 3), therefore we suggested that oligonucleotides labeled with dU^{DAB} could be used as promising photoregulatable molecular devices.[50, 52] When **ON5** was irradiated in PBS buffer, no significant spectral change could be detected with a conventional spectrophotometer due to the rapid thermal *cis*-to-*trans* transition of dU^{DAB} (Fig. S4A, Supporting Information).

It has previously been shown that the *cis-trans* isomerisation rate is faster in protic solvents due to protonation of dimethylamino group and consequently rotation about the N=N bond in the azonium tautomer.[51, 69] Hence, we attempted to observe changes in the absorption of **ON5** in dry DMSO, an aprotic solvent. Figure S4B shows spectral changes of **ON5** undergoing *cis-trans* isomerisation due to thermal relaxation, after irradiation at either 365 or 420 nm in dry DMSO.[70] The spectra of the *trans* isomer (blue line in Fig. S4B, Supporting Information) and *cis* isomer (orange line) are significantly different, showing clearly noticeable nπ* and ππ* bands at 377 nm and 447 nm, respectively. The complete thermal conversion back to *trans* isomer was achieved in the dark after 10 min at RT (Fig. S4B, Supporting Information). The same sample was irradiated again and exhibited complete recovery indicating a reversible and reproducible photoisomerisation process.

dU^{DAB} enhances duplex stability of the probes

The effect of dU^{DAB} on duplex stability was studied by UV thermal melting curves. We determined the T_m of dU^{DAB} containing strand displacement probes, **ON1:ON2**, **ON3:ON4**, and **ON3:ON5**, and the corresponding unmodified duplexes (Table 3). In the unmodified strands dU^{DAB} was replaced by 2'-OMe-U for **ON1** and dT for **ON4** and **ON5**.

In all cases incorporation of dU^{DAB} had a stabilizing effect on the duplex, causing an increase in T_m up to 11ºC (Table 3). The increase of T_m was greatest when the dU^{DAB} was incorporated in 2'-OMe-RNA (**ON1:ON2)**, and least when three dU^{DAB} monomers were incorporated into DNA (**ON3:ON5**). The duplex stabilizing effect of dU^{DAB} could be attributed to stacking interactions of azobenzene at uridine's 5' or 3' position with FAM at a nucleotide's 5' or 3' position.[54]

Table 3. Thermal denaturation temperatures of dU^{DAB} labeled ONs in PBS buffer, pH 7.4

	T_m (°C)
ON1(unmodified):ON2	57.0 ± 0.2
ON1:ON2	68.0 ± 0.6
ON3:ON4(unmodified)	54.9 ± 0.2
ON3:ON4	62.0 ± 0.3
ON3:ON5(unmodified)	54.0 ± 0.3
ON3:ON5	59.2 ± 0.3

Efficiency of quenching of dU^{DAB} in oligonucleotide probes

We measured the quenching ability of dU^{DAB} labeled oligonucleotides by preparing the corresponding duplex with FAM labeled complementary strands. When the two oligonucleotides are annealed, the FAM fluorophore and the dU^{DAB} quencher are held in close proximity causing the duplex to be non-fluorescent. We measured the fluorescence spectra of the oligonucleotides before and after annealing (Fig. S5, Supporting Information). **ON1:ON2** probe showed a significant quenching efficiency, up to 10-fold decrease of the fluorescence intensity (up to 90% quenching, Fig. S5A, Supporting Information). In contrast **ON3:ON4**, **ON3:ON5** exhibited lower quenching efficiency, with 75% and 83% quenching respectively (Fig. S5B and S5C, Supporting Information). The effective quenching of FAM fluorescence in the **ON1:ON2** duplex could be explained by higher duplex stability of 2'-OMe-RNA strand **ON1** with the DNA strand **ON2** (T_m 68 ^oC) as compared to that of DNA:DNA duplex of the **ON3:ON4** and **ON3:ON5** probes (62 ^oC and 59 ^oC, respectively). Nevertheless, incorporation of three dU^{DAB} monomers in the **ON3:ON5** probe**,** exhibited improved quenching as compared to **ON3:ON4** with one quencher.

Next, the double stranded probes **ON1:ON2**, **ON3:ON4**, and **ON3:ON5** were tested with single strand 35-mer **ON8** as the reaction target, which perfectly matched to the long strand of the probes, **ON1** and **ON3**. Figure 5A shows the kinetic curves for the double stranded oligonucleotides hybridized to the target oligonucleotide **ON8**, due to strand displacement. Complete dehybridization-hybridization reaction occurred for all probes after ca. 40 min at RT.

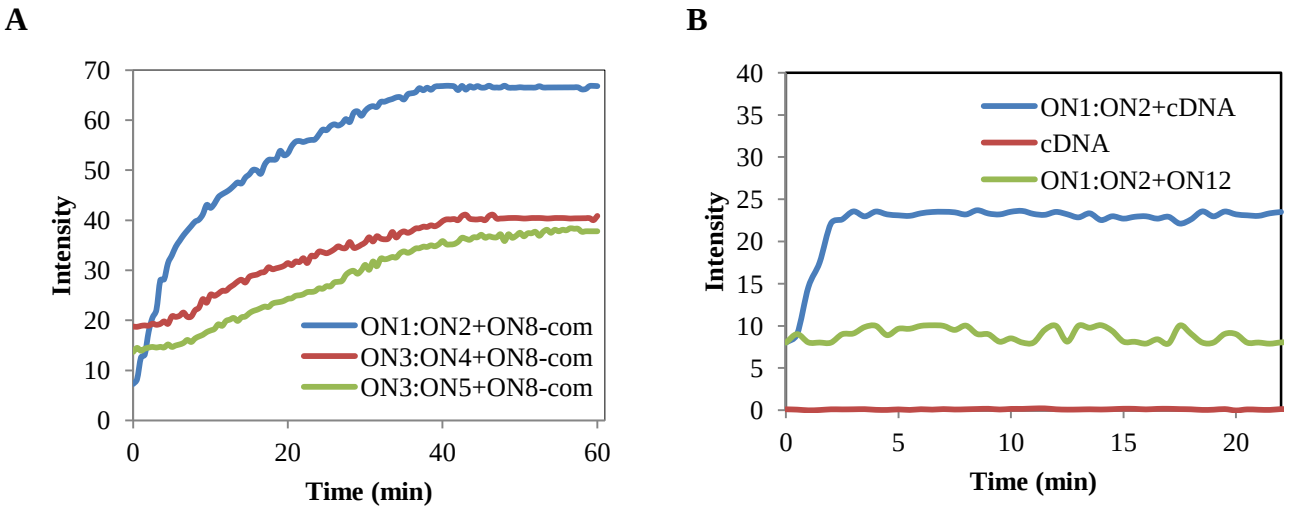

Figure 5 (A) Kinetics of displacement hybridization of double stranded probes **ON1:ON2**, **ON3:ON4** and **ON3:ON5** (1 µM) upon addition of a 35-mer DNA target **ON8** (1.5 µM). (B) Kinetics of **ON1:ON2** double stranded probe (1 µM) upon addition of a 35-mer cDNA target (150 ng/µL), and scrambled 35-mer DNA target **ON12** (1.5 µM). All reactions were preformed in PBS buffer, at room temperature, λ_{ex} 495 nm.

The background fluorescence intensity of the **ON1:ON2** probe, where the long strand of the probe was labeled with dU^{DAB} at 5'-end and the short strand labeled with FAM at 3'-end, was the lowest as expected, based on quenching efficiency data (90% quenching, Fig. S6, Supporting Information). When **ON8** target was added to the **ON1:ON2** probe**,** displacement of FAM- bearing strand by the target occurred resulting in 8.5-fold increase in fluorescence intensity (Fig. 5A). In comparison, when **ON8** target was added to the **ON3:ON4** and **ON3:ON5** probes, where the long strand of the probe was labeled with FAM at 5'-end and the short strand labeled with one or three dU^{DAB}, the

fluorescence intensity increased but to a lesser extent (3-fold), due to displacement of dU^{DAB} labeled strand and hybridization of FAM bearing strand to the target.

The smaller increase of fluorescence upon reaction of **ON3:ON4** and **ON3:ON5** probes vs. **ON1:ON2** probe, (3 vs. 8.5) is possibly due to quenching of FAM fluorescence by the nucleobases of the complementary target **ON8** after strand displacement for the **ON3:ON4** and **ON3:ON5** probes (Fig. 4). In contrast, upon displacement reaction of **ON2** from **ON1:ON2**, the FAM- bearing strand is released from the formed duplex to the medium.

In order to show the applicability of the double stranded probes for the detection of specific targets in homogeneous solution, we measured reaction kinetics of **ON1:ON2**, targeting a β-actin gene sequence, with a cDNA that was biochemically retro-synthesized from RNA extracted from human Hep G2 liver cancer cells (Fig. 5B). As controls we measured time-dependent fluorescence intensity of the cDNA alone, and of scrambled oligonucleotide **ON12** that was completely mismatched to the probe.

Upon cDNA addition at room temperature the fluorescence intensity of FAM increased almost immediately and reached the maximum after 2 min (Fig. 5B), indicating a rapid strand displacement reaction between double stranded probe and the DNA target. Nearly 3-fold fluorescence increase was observed indicating the formation of the desired ON2: β-actin gene sequence DNA duplex. Specific target recognition rather than spontaneous opening of the probe in the presence of any ON, was confirmed by the lack of change in fluorescence intensity upon addition of a scrambled 35-mer DNA to the **ON1:ON2** probe.

RT-PCR detection with double-stranded probe labeled with dU^{DAB}

The basic principle of quantitative PCR analysis by enzymatic hydrolysis of strand displacement probes is shown in Figure 6. The fluorescence of a FAM- bearing strand at 5'-end is quenched by a complementary short strand bearing dU^{DAB} at 3'-end. The FAM-labeled strand preferentially binds to the DNA target, in a strand displacement process and becomes relatively fluorescent. The probe is then digested by Taq polymerase during extention, releasing the fluorophore, and generating a more intense signal. The quencher oligonucleotide may show maximal quenching (through target annealing) below the standard PCR annealing temperature of ~60 ^{o}C, leading to a significant reduction in detection sensitivity. To improve the analytical quality of probes and ensure that the probe is annealed to the target, we have reduced the temperature of the annealing step to 47 ^{o}C and then the fluorescence detection step was preformed. The primers and the probe annealed to the target, and the cleavage of 6-FAM occurred during extention. Afterwards the temperature was increased allowing the Taq polymerase to complete polymerization by chain extention at 72^{o} C. This modified protocol produced signal generation with reduced background fluorescence.

We demonstrated the utilization of this method for the detection of the human β-actin gene. We used **ON3:ON4**, where a long strand **ON3**, labeled with FAM at the 5' end, and a short strand **ON4**, labeled with dU^{DAB} quencher at the 3' end. In addition we used the **ON3:ON5** PCR probe, where the short strand was labeled with three dU^{DAB} quenchers. An excess of the quencher strand was used to ensure optimal quenching of the duplex probe, setting the ratio to 1:2, where the long strand FAM- labeled (**ON3**) and dU^{DAB}- labeled short strand (**ON4, ON5**). By measuring fluorescence intensity of FAM during the annealing stage of every cycle, PCR can be followed in the real time format.

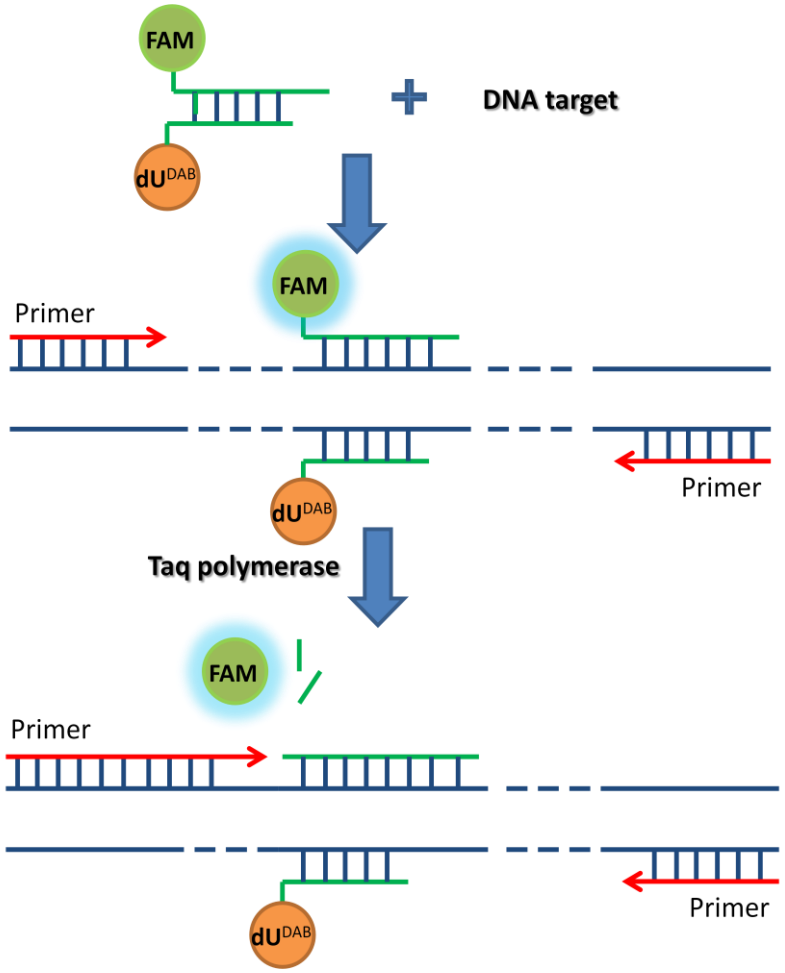

Figure 6 Schematic description of 5'-nuclease assay with a double stranded probe containing a FAM- bearing long strand at 5'-end and a short strand bearing dU^{DAB} at 3'-end.

First we preformed PCR reaction with 8 ng of the cDNA target and displacement probes **ON3:ON4** and **ON3:ON5**, and compared its sensitivity/efficiency performance to that of TaqMan probe labeled with DABCYL **ON11**. The PCR experiments were performed with **ON9** and **ON10** primers. Figure 7A shows linear dependence of relative fluorescence units (RFU) vs. cycles of amplification reaction.

As expected standard real-time detection curves were obtained, but no significant improvement in fluorescent signal was observed compared to **ON11**. The fluorescent signal crossed the threshold at cycle 18 for **ON11** and cycles 21 and 22 for the two studied strand displacement probes, **ON3:ON4** and **ON3:ON5**, respectively

(logarithmic amplification curves shown in Fig S9, Supporting Information). However, the **ON3:ON5** probe, where the short strand was labeled with three dU^{DAB} quenchers performed better than the probe with one quencher, **ON3:ON4**.

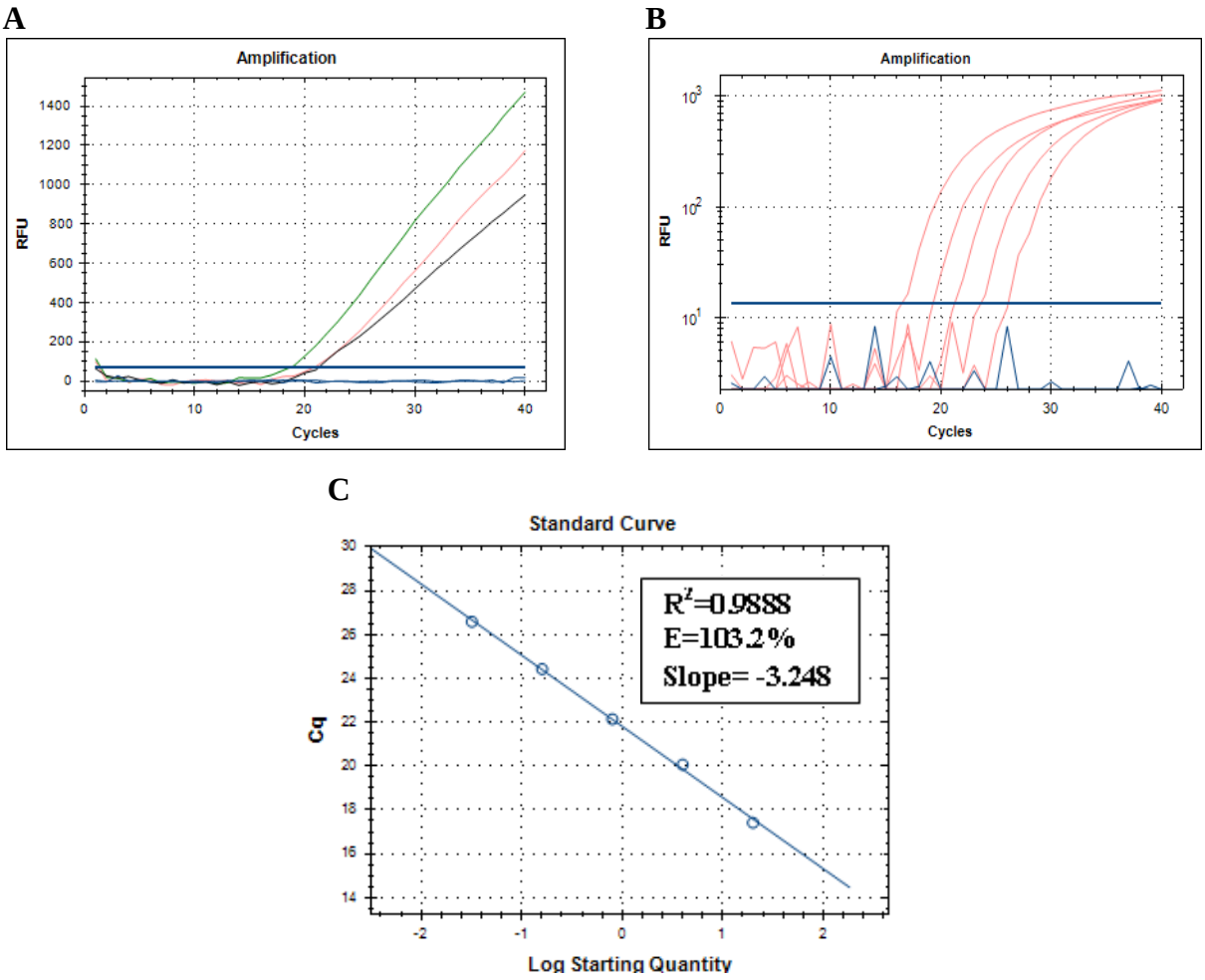

Figure 7 (A) Linear amplification curves (RFU vs. cycle) of **ON3:ON4** (gray line) and **ON3:ON5** (pink line) double stranded probes labeled with dU^{DAB} quenchers in PCR assay compared to that of the TaqMan probe labeled with DABCYL, **ON11** (green line) (8 ng cDNA). (B) Logarithmic scale amplification curves (log RFU vs. cycle) of **ON3:ON5** double stranded probe in qPCR analysis of cDNA (20 ng, 4 ng, 0.8 ng, 0.16 ng and 0.032 ng, pink lines) obtained from human Hep G2 liver cells; no template control (blue line). (C) Standard curve showing RT-PCR efficiency of **ON3:ON5** double stranded probe (number of cycle vs. log of concentration).

This improvement in performance is manifested as an increase of maximum fluorescence intensity signal (1471 RFU for **ON3:ON5** vs. 948 RFU for **ON3:ON4**) and decrease in cycle number at which the fluorescent signal emerges from the background.

The background fluorescence of strand displacement probes is not higher than that of the standard TaqMan probe **ON11**, due to having FAM attached closer to dU^{DAB} quencher (around 80 RFU).

Next, five reactions were performed with the **ON3:ON5** double stranded probe and serially diluted template cDNA (20 ng, 4 ng, 0.8 ng, 0.16 ng and 0.032 ng). Figure 7B shows the logarithmic amplification curves for a cDNA dilution series. The results fit well across the range of concentration tested. Moreover, the standard curve, that indicates PCR efficiency exhibited very close to a 2-fold change for each cycle (~100% efficiency) (Fig. 7C).

Taken together, these data indicate that dU^{DAB} displacement probes are capable of producing high-quality quantitative measurements.

RT-PCR detection with a TaqMan probe labeled by one or two dU^{DAB} quenchers

A widely used probe for quantitative PCR is a TaqMan probe, oligonucleotide containing one fluorophore and one quencher.[26, 27] The probe is complementary to the target that is amplified, and is susceptible of 5'→3' degradation by the exonuclease activity of DNA polymerase, resulting in increase in fluorescence intensity.

Properly designed probes should have low background and high fluorescence signal. Approaches leading to a background fluorescence decrease of the TaqMan probe include the moving of a quencher from a terminal to an internal position or by incorporating additional quenchers. A short distance between the fluorophore and the quencher would give more efficient quenching of the probe fluorescence (Fig. 8). Hence **ON6** and **ON7** TaqMan based probes labeled with one or two dU^{DAB} quenchers were prepared and investigated for their ability to detect human β-actin target sequence in the 5'-nuclease

PCR assay. We used the same method for PCR as for double stranded displacement probes and the same primers, **ON9** and **ON10**.

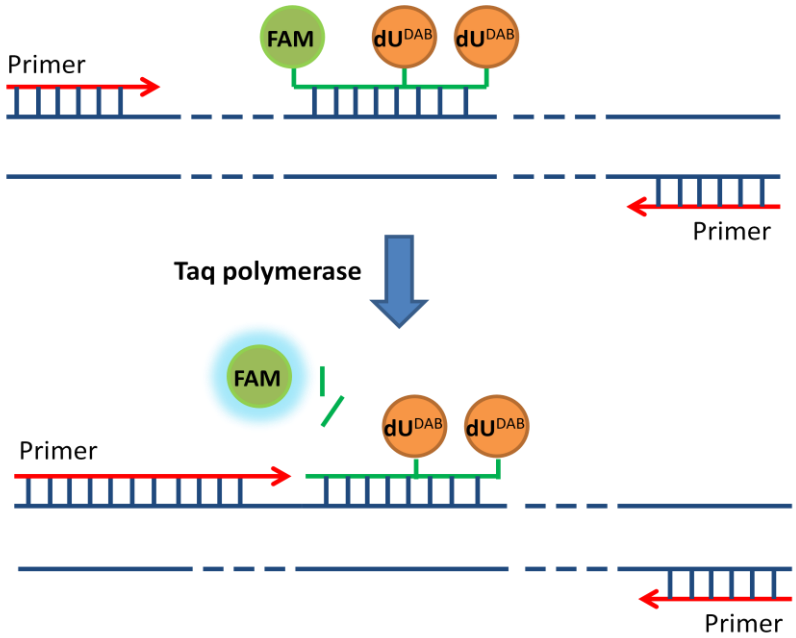

Figure 8 Schematic description of 5'-nuclease assay with doubly labeled dU^{DAB} TaqMan probe.

Fluorescence was measured at the end of the extention step, where the fluorescence is the highest (unlike in strand displacement approach). Figure 9A shows the results of PCR reaction with 8 ng of the cDNA target in presence of **ON6** or **ON7** probe in comparison to TaqMan probe labeled with DABCYL, **ON11** (linear dependence). Probe **ON6** resulted in slight increase in reporter maximum fluorescence intensity compared to **ON11** (2817 RFU for **ON6** and 2718 RFU for **ON11**). However, probe **ON7** labeled with two dU^{DAB} quenchers produced a much lower fluorescent signal, presumably due to the reduced probe degradation in the course of the PCR (749 RFU).

Next, we selected **ON6** probe to test in qPCR template serial dilutions when compared to **ON11** labeled with DABCYL. Figure 9B shows the logarithmic amplification curves of **ON6** for a cDNA dilution series. The signal to noise ratio, threshold level, was

improved as compared to **ON11** (Fig. 9D) with enhancement of the fluorescent signal (1248 RFU vs. 1138).

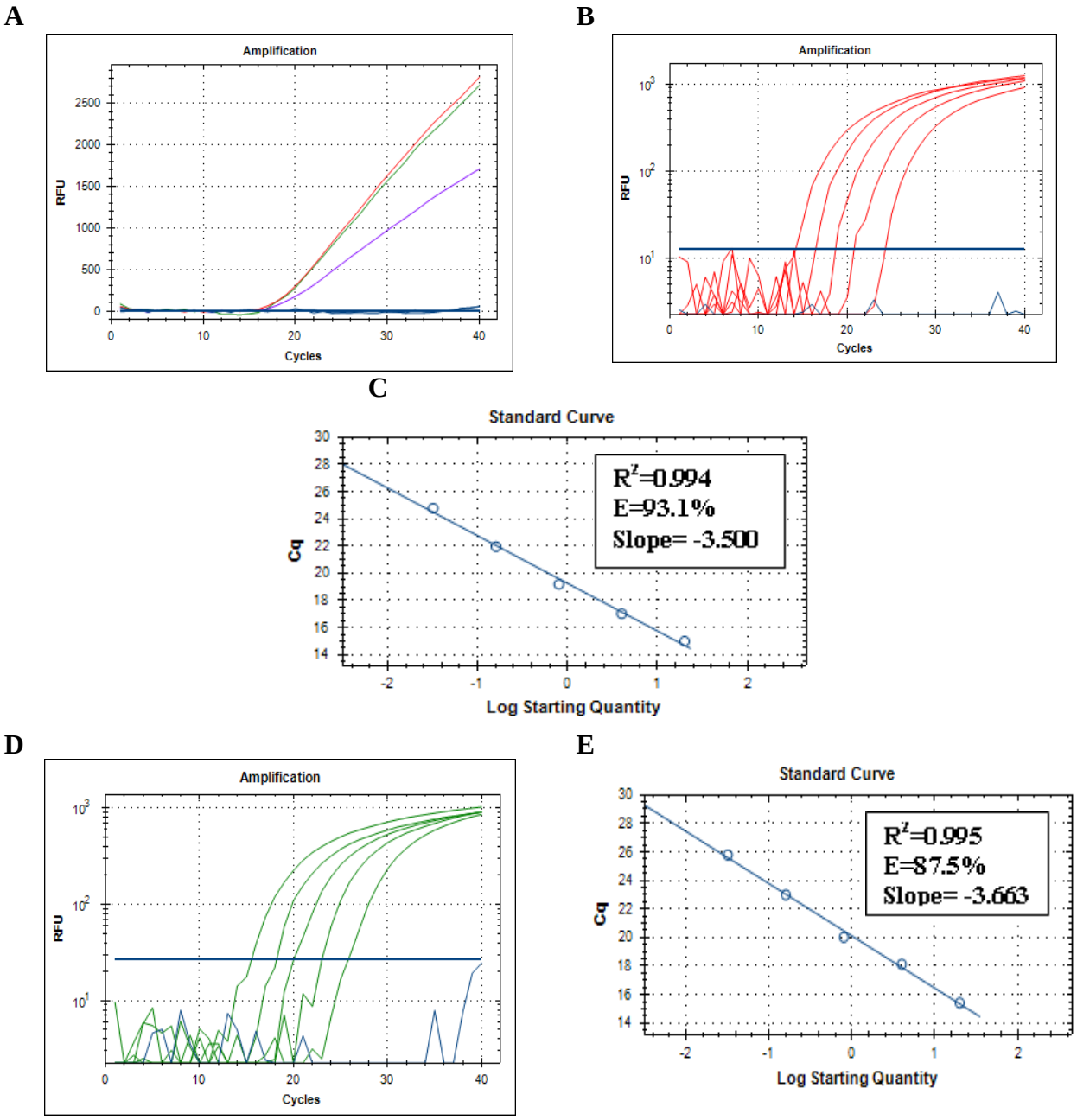

Figure 9 (A) Linear amplification curves (RFU vs. cycle) of **ON6** (red line) and **ON7** (purple line) TaqMan probes, labeled with dU^{DAB} quenchers in PCR assay compared to that of the TaqMan probe labeled with DABCYL, **ON11** (green line).using 8 ng cDNA. (B) Logarithmic scale amplification curves (log RFU vs. cycle) of **ON6** probe in qPCR analysis of cDNA (20 ng, 4 ng, 0.8 ng, 0.16 ng and 0.032 ng, red lines) obtained from human Hep G2 liver cells; no template control (blue line). (C) Standard curve showing rtPCR efficiency of **ON6** double stranded probe (number of cycle vs. log of concentration). (D**) ON11** in qPCR analysis of cDNA (20 ng, 4 ng, 0.8 ng, 0.16 ng and 0.032 ng, green lines) obtained from human Hep G2 liver cells; no template control (blue line). (E) Standard curve showing rtPCR efficiency of **ON11** double stranded probe (number of cycle vs. log of concentration).

Furthermore, these results revealed a linear measuring range over at least five concentrations with better efficiency of PCR reaction in comparison to **ON11** labeled with a DABCYL quencher (93.1% for **ON6** vs. 87.5% for **ON11**). Control experiments carried out without cDNA showed that the dU^{DAB} labeled TaqMan probes avoided false-positive signaling in PCR assay. These results indicate that dU^{DAB} modified TaqMan probes may be suitable for gene quantification in real-time detection.

Conclusions

A non-fluorescent, DABCYL based, photoswitchable nucleoside **1** (dU^{DAB}) was synthesized and incorporated into oligonucleotides at various positions, to construct probes for fluorescent-based DNA detection assays. X-ray crystal structure of dU^{DAB}, nucleoside confirmed that it is a very good structural mimic of thymidine. The azobenzene moiety of dU^{DAB} and of the dU^{DAB} triply labeled oligonucleotide **ON5** underwent photoisomerisation upon irradiation, confirming its function as a photoswitch. The photoswitchable device presented here includes also a reporter for the photocontrol of DNA/RNA duplex formation. Yes additional studies are required to establish its potential. In particular, the required studies include determination of the timescale of potoisomerisation of the strand labeled with dU^{DAB} in DMSO and water and to monitoring duplex dissociation and formation. These studies will be reported in due course.

In addition, dU^{DAB} was used to prepare strand displacement probes bearing dU^{DAB} at 5'-end or 3'-end of the quencher strand and FAM on the fluorescent strand, as well as TaqMan probes labeled with one or two dU^{DAB} and FAM. These probes were used successfully in FRET applications for real-time detection of a DNA target. With the double stranded probe **ON1:ON2** where the long strand was labeled with dU^{DAB} and the

short strand with FAM, we were able to detect small amounts of β-actin DNA target in homogeneous solution of cDNA (150 ng/μL). **ON3:ON5** strand displacement probe where the quencher strand was labeled with three dU^{DAB} exhibited excellent PCR efficiency (~100%). With dU^{DAB} modified TaqMan probes we showed more significant PCR efficiency as compared to **ON11**, probe with commercial quencher DABCYL (93% for **ON6** vs. 87% for **ON11**) with enhancement of the fluorescent signal. dU^{DAB} quencher significantly stabilizes DNA duplexes (ΔT_m 5-11 ^oC). This may facilitate the design of short, more specific probes for rtPCR detection that are readily synthesized, cheaper and less complex than standard TaqMan probes.

Experimental

General information: Reagents and solvents were purchased from commercial sources and were used without further purification. All moisture sensitive reactions were carried out in flame-dried reaction flasks with rubber septa, and the reagents were introduced with a syringe. All reactants in moisture sensitive reactions were dried overnight in a vacuum oven. Progress of reactions was monitored by TLC on precoated Merck silica gel plates (60F-254). Visualization was accomplished by UV light. Medium pressure chromatography was carried out using automated flash purification system (Biotage SP1 separation system, Uppsala, Sweden). Compounds were characterized by nuclear magnetic resonance using Bruker AC-200, DPX-300 and DMX-600 spectrometers. ^1H NMR spectra were measured at 200, 300 and 600 MHz. Phosphoramidite monomer was characterized also by ^{31}P NMR in CD_3CN, using 85% aq. H_3PO_4 as an external reference on Bruker AC-200, at 80 MHz. Chemical shifts are expressed in ppm, downfield from Me_4Si (TMS), used as internal standard. Compounds were analyzed under ESI (electron spray ionization) conditions on a Q-TOF micro-instrument (Waters, UK). Unmodified oligonucleotides were purchased from Integrated DNA Technologies

(Coralville, Iowa, USA). Modified oligonucleotides were synthesized by standard automated solid-phase method on an AKTA OligoPilot (GE healthcare) an ABI DNA/RNA synthesizer (Forster City, USA). MALDI-TOF mass spectra of oligonucleotides were measured with mass spectrometer in a negative ion mode with THAP matrix. Absorption spectra were measured on a UV-2401PC UV-VIS recording spectrophotometer (Shimadzu, Kyoto, Japan). Emission spectra were measured using Cary Eclipse Fluorescence Spectrophotometer. Absorption and fluorescence spectra were recorded in PBS buffer containing NaC1 (8.0 g), KC1 (0.2 g), Na_2HPO_4 (1.15 g), KH_2PO_4 (0.2 g), in water (100 mL, pH 7.4).

Synthesis

***N*,*N*-Dimethyl-4-((4-(4,4,5,5-tetramethyl-1,3,2-dioxaborolan-2-yl)phenyl)azo) aniline, 5**

A solution containing 4-(4,4,5,5-tetramethyl-1,3,2-dioxaborolan-2-yl)aniline (1 g, 4.56 mmol), water (10 mL) and concentrated HCl (1.5 mL) was cooled to 0 ^{o}C. Sodium nitrite (330 mg, 4.78 mmol) in 15 mL of water was then added dropwise keeping the temperature below 20 ^{o}C. After 30 min, *N*,*N*-dimethylaniline (567 mg, 4.68 mmol) in 1 mL of acetic acid was added at 0 ^{o}C. The solution was stirred for 30 min at 0 ^{o}C and then, allowed to reach the room temperature. The product precipitated from the solution after neutralization to pH ~ 7 with 20 % NaOH. The brown solid was filtered and washed, first, with cold water and then with cold methanol. The product was further purified by silica gel chromatography (CH_2Cl_2:MeOH, 95:5) to give 330 mg (21% yield) of an orange powder. ^{1}H NMR ($CDCl_3$, 400 MHz) δ 7.90 (m, 4H), 7.82 (d, *J* = 7.4 Hz, 2H), 6.76 (d, *J* = 7.4 Hz, 2H), 3.09 (s, 6H), 1.36 (s, 12H) ppm. ^{13}C NMR ($CDCl_3$, 100 MHz) δ 155.1, 152.6, 143.8, 135.5, 125.1, 121.4, 111.5, 83.9, 40.3, 29.7, 24.9 ppm.

HRMS (ESI-MS) *m/z*: calculated for $C_{20}H_{27}BN_3O_2$: 352.223 (MH^+), found: 352.221 (MH^+).

5-(4-(4-(Dimethylamino)azobenzene)-2'-deoxy-5'-*O*-(4,4'-dimethoxytrityl)uridine, 7

To a solution of 5-*I*-5'-*O*-(4,4'-dimethoxytrityl)uridine, **6** (600 mg, 0.91 mmol) in Water:acetonitrile (6:3 mL) under nitrogen was added **5** (401 mg, 1.14 mmol), $Pd(OAc)_2$ (10.3 mg, 0.046 mmol), TPPTS (125 mg, 0.22 mmol) and Na_2CO_3 (63 mg, 2.73 mmol). The mixture was stirred under reflux for 2 h and monitored by TLC (8.5:1.5, DCM:MeOH). The solvents were evaporated. The crude orange residue was separated on a silica gel column (3 % MeOH in DCM). Product **7** was obtained as an orange solid (450 mg, 65 %). ^{1}H NMR (Acetone-d_6, 600 MHz) δ 7.89 (s, 1H), 7.83 (d, *J* = 8.4 Hz, 2H), 7.62 (d, *J* = 6.6 Hz, 2H), 7.53 (d, *J* = 6.6 Hz, 2H), 7.44 (d, *J* = 6.6 Hz, 2H),7.28 (m, 4H), 7.25 (m, 2H), 7.19 (m, 1H), 6.85 (d, *J* = 7.1 Hz, 2H), 6.77 (d, *J* = 8.5 Hz, 4H), 6.40 (m, , 1H), 4.59 (m, 1H), 4.13 (m, 1H), 3.72 (s, 3H), 3.71 (s, 3H), 3.35 (m, 2H), 3.10 (s, 6H), 2.46 (m, 2H) ppm. ^{13}C NMR (Acetone-d_6, 150 MHz) 162.1, 159.6, 159.5, 153.7, 152.8, 150.6, 145.8, 144.3, 140.9, 138.1, 136.7, 136.5, 135.2, 130.9, 130.8, 130.7, 129.6, 129.0, 128.9, 128.6, 127.6, 127.5, 125.6, 122.5, 114.8, 114.0, 113.9, 113.8, 112.4, 87.2, 86.1, 72.4, 64.5, 55.5, 46.9, 41.4, 40.3 ppm. HRMS (ESI-MS) *m/z*: calculated for $C_{44}H_{44}N_5O_7$: 754.324 (MH^+), found: 754.327 (MH^+).

5-(4-(4-(Dimethylamino)azobenzene)-2'-deoxy-5'-*O*-(4,4'-dimethoxytrityl) uridine-3'-*O*-(2-cyanoethyl-N,N-diisopropyl)phosphoramidite 8

A 0.45 M solution of tetrazole (0.133 mmol, 0.300 mL) in anhydrous acetonitrile was added with stirring under a flow of argon, to a solution of **7** (100 mg, 0.133 mmol) in anhydrous acetonitrile (0.665 mL), followed by 2-cyanoethyl-*N,N,N',N'*-tetraisopropyl phosphoramidite (0.133 mmol, 42 µL). TLC analysis showed that the reaction was

completed within 1 h, with the formation of the product as two diastereoisomers. The precipitated diisopropylammonium tetrazolide was removed by filtration and the solution diluted with anhydrous acetonitrile (0.665 mL), to give 0.1 M solution of **8**. The solution was immediately used in the phosphorylation step on an automated oligonucleotide synthesizer, without further purification. Presence of the product was checked by phosphorus NMR analysis and mass spectroscopy. ^{31}P NMR ($CDCl_3$, 80 MHz) δ 149.49, 149.22 ppm. MS (ESI-MS) *m/z*: calculated for $C_{53}H_{61}N_7O_8P$: 954 (MH^+), found: 954 (MH^+).

5-(4-(4-(Dimethylamino)azobenzene)-2'-deoxy-uridine-dU^{DAB}, 1

To a solution of **7** (55 mg, 0.07 mmol) in dichloromethane (1 mL) was added 3% trichloroacetic acid in dichloromethane (2 mL) and the mixture was stirred for 30 min at room temperature. The resulting mixture was evaporated and purified by silica gel chromatography (DCM:MeOH, 8:2), to yield **9** as an orange solid (30 mg, 85 % yield). ATIR (ZnSe): *v* 2924, 2853, 2359, 1717, 1627, 1602, 1515, 1469, 1417, 1393, 1366, 1278, 1226, 1141, 1097, 1060, 1024, 912, 943, 822, 720, 700 cm^{-1}. ^{1}H NMR (Acetone-d_6, 600 MHz) δ 10.1 (br. s, 1H), 8.54 (s, 1H), 7.82 (m, 6H), 6.85 (d, *J* = 11.1 Hz, 2H), 6.41 (t, *J* = 6.2 Hz, 1H), 4.59 (m, 1H), 4.03 (m, 1H), 3.88 (m, 2H), 3.11 (s, 6H), 2.44 (m, 1H), 2.36 (m, 1H) ppm. ^{13}C NMR (Acetone-d_6, 150 MHz) 162.6, 153.7, 152.8, 150.6, 144.3, 140.9, 139.4, 135.8, 129.3, 125.6, 122.5, 114.0, 112.4, 88.8, 86.2, 71.8, 62.4, 41.7, 40.3 ppm. HRMS (ESI-MS) *m/z*: calculated for $C_{23}H_{26}N_5O_5$: 452.193 (MH^+), found: 452.193 (MH^+).

Oligonucleotide Synthesis, Work-up and Purification. The oligonucleotide probes were assembled by a DNA/RNA synthesizer using the and by phosphoramidite method. CPGs (3 µmol, pore size 500 Å), commercially available phosphoramidites were used.

6-Carboxyfluorescein (6-FAM) phosphoramidite and the synthesized dU^{DAB} modified nucleoside phosphoramidite **8** were used at 0.1 M in dry acetonitrile. The ONs were cleaved from the support with 1:1 (v/v) 33% NH_4OH and 33% methylamine in ethanol at 65 ^{o}C, for 10 min. The crude product was purified by RP-HPLC on C-18 column, and eluted with a linear gradient of 0.1 M TEAA (pH = 7) and acetonitrile, from 5% to 40% acetonitrile, over 30 min, at a flow rate of 3 mL/min. The oligomers were converted to the corresponding sodium salt using CM Sephadex C-25 equilibrated in NaCl and washed well with water. The identity of the oligomers was determined by MALDI-TOF mass spectroscopy: **ON1** calcd *m/z* for $C_{211}H_{255}N_{72}O_{134}P_{19}Na$ 6552.02, found 6552.56, **ON2** calcd *m/z* for $C_{172}H_{190}N_{57}O_{102}P_{16}$ 5180.72, found 5182.12, **ON3** calcd *m/z* for $C_{200}H_{223}N_{68}O_{118}P_{19}Na$ 6075.84, found 6078.17, **ON4** calcd *m/z* for $C_{148}H_{173}N_{54}O_{86}P_{14}Na$ 4538.70, found 4540.32**,** **ON5** calcd *m/z* for $C_{184}H_{203}N_{62}O_{86}P_{15}Na$ 5255.90, found 5258.13, **ON6** calcd *m/z* for $C_{223}H_{255}N_{73}O_{125}P_{20}Na$ 6597.05, found 6596.89, **ON7** calcd *m/z* for $C_{236}H_{258}N_{76}O_{125}P_{20}Na$ 6798.08, found 6795.43.

Calculation of Oligonucleotides' Extinction Coefficients and Concentration Concentrations of oligonucleotides were calculated using the following extinction coefficients (OD260/μmol): The individual extinction coefficients at 260 nm used were: ε_{dT} = 8400 M^{-1} cm^{-1}, ε_{dC} = 7050 M^{-1} cm^{-1}, ε_{dG} = 12 010 M^{-1} cm^{-1}, ε_{dA} = 15 200 M^{-1} cm^{-1}, $\varepsilon_{U\text{-}2'\text{-}OMe}$ = 10 000 M^{-1} cm^{-1}, $\varepsilon_{C\text{-}2'\text{-}OMe}$ = 9050 M^{-1} cm^{-1}, $\varepsilon_{G\text{-}2'\text{-}OMe}$ = 13 700 M^{-1} cm^{-1}, $\varepsilon_{A\text{-}2'\text{-}OMe}$ = 15 400 M^{-1} cm^{-1}, $\varepsilon_{dU}{}^{DAB}$ = 14 800 M^{-1} cm^{-1}, ε_{DABCIL} = 11 100 M^{-1} cm^{-1}, ε_{FAM} = 20 960 M^{-1} cm^{-1}. The extinction coefficients for the modified oligonucleotides were approximated by the linear combination of the extinction coefficients of the natural nucleotides and the extinction coefficient of the modified nucleoside. To account for the base stacking interactions, this linear combination was multiplied by 0.9 to give the final extinction coefficients for the oligomers. The extinction coefficients of the duplexes (ε_D)

are less than the sum of the extinction coefficients of their complementary strands (ε_{S1}, ε_{S2}), due to hypochromic effect that should be taken into account.[71] Therefore, the extinction coefficients were calculated by the following equation:

$$\varepsilon_D = (1\text{-}h_{260nm})(\varepsilon_{S1} + \varepsilon_{S2})$$

$$h_{260nm} = 0.287f_{AT} + 0.059f_{GC}$$

Where f_{AT} and f_{GC} are the fractions of the AT and GC base pairs, respectively.

Hybridization of Oligonucleotides. Solutions of labeled single-strands were mixed at room temperature with an equimolar amount of the complementary single strand oligonucleotides in PBS buffer (pH 7.4). Samples were hybridized by heating to 90 ºC for 5 min and subsequently allowed to cool to room temperature over 2 h prior to measurements.

UV/Vis Spectroscopy. The absorption spectra of **1** were measured in dichloromethane, DMSO, and acetone at 15 µM. Absorption spectra of the oligonucleotide probes were measured in DMSO and PBS buffer containing NaC1 (8.0 g), KC1 (0.2 g), Na_2HPO_4 (1.15 g), KH_2PO_4 (0.2 g), in water (100 mL, pH 7.4). The concentrations of the oligonucleotides were in the range of 10 µM. Samples were measured in a 10 mm quartz cell.

Isomerisation studies. *Trans*-to-*cis* photoisomerization of nucleoside **1** was monitored by UV/Vis spectroscopy. A 15 µM solution of **1** in dichloromethane was irradiated with UV-light at room temperature using a UV hand held lamp (6 Watt, 366 nm) at a distance of approximately 3 cm. The spectral change for absorption maximum peak at 420 nm and were monitored with the time course of irradiation. While the *cis*-to-*trans* isomerization was achieved by leaving the samples at the dark at room temperature thermally was monitored and confirmed by retrieving the maximum absorption band at

549 nm. *Cis*-to- *trans* photoisomerization of ON5 in DMSO (10 μM) was measured by irradiation with UV (350 nm) or visible (420 nm) light from 150 W Xenon lamp through a 5 nm slit at room temperature by placing a quarts cuvette containing the sample in the light path of a fluorescence spectrophotometer. Before the experiment DMSO were dried with molecular sieves overnight and we confirmed if the absorption of the sample at 440 nm did not change over 30 min in the dark.

Fluorescence Measurements of oligonucleotides. The fluorescence measurement conditions of oligonucleotides included 5 nm slit. λ_{ex} = 495, λ_{em} = 500-700 nm range. The concentration of the samples was 1 μM. Samples were measured in a 10 mm quartz cell.

PCR Systems. Primers and probes were designed using ABI Primer Express 3.0 program (Applied Biosystem Foster City CA, USA). A 103 bp segment from human β-actin gene (nucleotides 1150-1206) was amplified using primer **ON10** and **ON11**. All real –time PCRs was performed on a CFX-96 (Bio-Rad, USA) Each PCR reaction (20 μL) containing 10 μL of 2×TaqMan PCR Mix (Applied Biosystem Foster City CA, USA); 0.4 μM primers; for double stranded probes: 0.1 μM long strand labeled with FAM and 0.2 μM for short strand labeled with dU^{DAB}; for TaqMan probe 0.2 μM and 1 μM cDNA solution. In the no template control reactions cDNA was replaced with water. Each reaction mixture (3×20 μM) was transferred to a 96-well plate, sealed with a plastic foil, and centrifuged to remove the bubbles. The temperature protocol of PCR included initial denaturation and enzyme activation (95^{o} C, 15 min) followed by 40 cycles of denaturation (95^{o} C, 30 sec), annealing (47^{o} C, 30 sec) and elongation (72^{o} C, 1 min). Fluorescence readout was performed at annealed temperature for double-stranded probes and in the end of extention step.

Thermal denaturation measurements (T_m). The T_m values of duplexes were measured in PBS buffer (pH 7.4) at 1 µM concentrations. The absorbance of the samples was monitored at 260 nm and the temperature ranged from 20 to 85 ºC with heating rate of 1 ºC/min.

X-Ray Crystallography. Crystals of dU^{DAB}, **1,** were grown from a concentrated dichloromethane solution by slow diffusion of hexane. An orange plate was mounted on a glass fiber. Data were collected at 100 K on Bruker Apex2. Program(s) used to solve and refine structure: *SHELXS97* (Sheldrick, 1990), *SHELXL97* (Sheldrick, 1997). The crystallographic and refinement parameters for **1** are given in Table S1 in supporting information. CCDC number 972500 contains the supplementary crystallographic data for this paper. These data can be obtained free of charge from the Cambridge Crystallographic Data Centre *via* www.ccdc.cam.ac.uk/data_request/cif.

Acknowledgments

We thank to Dr. Linda J. W. Shimon, Head, X-ray Crystallography Laboratory Chemical Research Support Unit Weizmann Institute of Science, Israel, for performing X-Ray crystallography analysis.

References

1. K. K. Karlsen, A. Pasternak, T. B. Jensen and J. Wengel, *ChemBioChem*, 2012, **13**, 590-601.
2. F. Hoevelmann, L. Bethge and O. Seitz, *ChemBioChem*, 2012, **13**, 2072-2081.
3. I. V. Astakhova, T. S. Kumar and J. Wengel, *Collect. Czech. Chem. Commun.*, 2011, **76**, 1347-1360.
4. M. Segal and B. Fischer, *Org. Biomol. Chem.*, 2012, **10**, 1571-1580.
5. M. Segal, E. Yavin, P. Kafri, Y. Shav-Tal and B. Fischer, *J. Med. Chem.*, 2013, **56**, 4860-4869.

6. K. J. Livak, S. Flood, J. Marmaro, W. Giusti and K. Deetz, *Genome Res.*, 1995, **4**, 357-362.

7. N. Venkatesan, Y. J. Seo and B. H. Kim, *Chem. Soc. Rev.*, 2008, **37**, 648-663.

8. C. M. McKeen, L. J. Brown, J. T. Nicol, J. M. Mellor and T. Brown, *Org. Biomol. Chem.*, 2003, **1**, 2267-2275.

9. D. Whitcombe, J. Theaker, S. P. Guy, T. Brown and S. Little, *Nat. Biotechnol.*, 1999, **17**, 804-807.

10. G. H. Reed, J. O. Kent and C. T. Wittwer, *Pharmacogenomics*, 2007, **8**, 597-608.

11. M. J. Heller, *Annu. Rev. Biomed. Eng.*, 2002, **4**, 129-153.

12. A. Okamoto, K. Tanaka, T. Fukuta and I. Saito, *J. Am. Chem. Soc.*, 2003, **125**, 9296-9297.

13. K. Miyata, R. Tamamushi, A. Ohkubo, H. Taguchi, K. Seio, T. Santa and M. Sekine, *Org. Lett.*, 2006, **8**, 1545-1548.

14. P. Bosch, A. Fernandez-Arizpe, J. L. Mateo, A. E. Lozano and P. Noheda, *J Photochem. Photobiol. A*, 2000, **133**, 51-57.

15. R. B. Macgregor and G. Weber, *Nature*, 1986, **319**, 70-73.

16. G. Weber and F. J. Farris, *Biochemistry*, 1979, **18**, 3075-3078.

17. K. Yamana, T. Mitsui, H. Hayashi and H. Nakano, *Tetrahedron Lett.*, 1997, **38**, 5815-5818.

18. K. Namba, A. Osawa, S. Ishizaka, N. Kitamura and K. Tanino, *J. Am. Chem. Soc.*, 2011, **133**, 11466-11469.

19. L. J. Kricka and P. Fortina, *Clin. Chem.*, 2009, **55**, 670-683.

20. J. Shinar, *Organic Light-Emitting Devices*, Springer, New York, 1st edn., 2004.

21. B. Valeur, *Molecular Fluorescence: Principles and Applications*, Wiley-VCH, Weinheim 2002.

22. Q. Li, G. Luan, Q. Guo and J. Liang, *Nucleic Acids Res.*, 2002, **30**, 5e.

23. W. Liu and D. A. Saint, *Anal. Biochem.*, 2002, **302**, 52-59.

24. D.-M. Kong, Y.-P. Huang, X.-B. Zhang, W.-H. Yang, H.-X. Shen and H.-F. Mi, *Anal. Chim. Acta*, 2003, **491**, 135-143.

25. S. Tyagi and F. R. Kramer, *Nat. Biotechnol.*, 1996, **14**, 303-308.

26. L. G. Lee, C. R. Connell and W. Bloch, *Nucleic Acids Res.*, 1993, **21**, 3761-3766.

27. K. J. Livak, S. J. Flood and J. Marmaro, Method for detecting nucleic acid amplification using self-quenching fluorescence probe, Google Pat.1996.

28. W. Shengqi, W. Xiaohong, C. Suhong and G. Wei, *Anal. Biochem.*, 2002, **309**, 206-211.

29. J. R. Lakowicz, *Principles of fluorescence spectroscopy*, Springer, Baltimore, 3th edn., 2009.

30. D. Proudnikov, V. Yuferov, Y. Zhou, K. S. LaForge, A. Ho and M. J. Kreek, *J. Neurosci. Methods*, 2003, **123**, 31-45.

31. A. Stakheev, D. Y. Ryazantsev, T. Y. Gagkaeva and S. Zavriev, *Food Control*, 2011, **22**, 462-468.

32. C. J. Yang, H. Lin and W. Tan, *J. Am. Chem. Soc.*, 2005, **127**, 12772-12773.

33. T. Gunnlaugsson, M. Nieuwenhuyzen, L. Richard and V. Thoss, *J. Chem. Soc., Perkin Trans. 2*, 2002, 141-150.

34. T. Gunnlaugsson, M. Nieuwenhuyzen, L. Richard and V. Thoss, *Tetrahedron Lett.*, 2001, **42**, 4725-4728.

35. P. Felderbauer, J. Schnekenburger, R. Lebert, K. Bulut, M. Parry, T. Meister, V. Schick, F. Schmitz, W. Domschke and W. E. Schmidt, *J. Med. Genet.*, 2008, **45**, 507-512.

36. J. Beythien and P. D. White, *Tetrahedron Lett.*, 2005, **46**, 101-104.

37. S. Tyagi, F. R. Kramer and P. M. Lizardi, Detectably labeled dual conformation oligonucleotide Probes, Assays and Kits, EP Patent 0,745,6902008.

38. Q. Xiao, R. T. Ranasinghe, A. M. Tang and T. Brown, *Tetrahedron*, 2007, **63**, 3483-3490.

39. T. Ikeda and T. Ube, *Mater. Today*, 2011, **14**, 480-487.

40. F. Ercole, T. P. Davis and R. A. Evans, *Polym. Chem.*, 2010, **1**, 37-54.

41. T. Fukaminato, M. Tanaka, T. Doi, N. Tamaoki, T. Katayama, A. Mallick, Y. Ishibashi, H. Miyasaka and M. Irie, *Photochem. Photobiol. Sci.*, 2010, **9**, 181-187.

42. A. A. Beharry and G. A. Woolley, *Chem. Soc. Rev.*, 2011, **40**, 4422-4437.

43. M. Volgraf, P. Gorostiza, S. Szobota, M. R. Helix, E. Y. Isacoff and D. Trauner, *J. Am. Chem. Soc.*, 2007, **129**, 260-261.

44. B. Schierling, A.-J. Noël, W. Wende, E. Volkov, E. Kubareva, T. Oretskaya, M. Kokkinidis, A. Römpp, B. Spengler and A. Pingoud, *Proc. Nat. Acad. Sci.*, 2010, **107**, 1361-1366.

45. F. Zhang, K. A. Timm, K. M. Arndt and G. A. Woolley, *Angew. Chem., Int. Ed.*, 2010, **49**, 3943-3946.

46. F. Bonardi, G. London, N. Nouwen, B. L. Feringa and A. J. Driessen, *Angew. Chem.*, 2010, **122**, 7392-7396.

47. C. Hoppmann, S. Seedorff, A. Richter, H. Fabian, P. Schmieder, K. Rück Braun and M. Beyermann, *Angew. Chem., Int. Ed. Engl.*, 2009, **48**, 6636-6639.

48. A. Yamazawa, X. Liang, H. Asanuma and M. Komiyama, *Angew. Chem., Int. Ed.*, 2000, **39**, 2356-2357.

49. X. Liang, H. Nishioka, N. Takenaka and H. Asanuma, *ChemBioChem*, 2008, **9**, 702-705.

50. H. Asanuma, X. Liang, T. Yoshida and M. Komiyama, *ChemBioChem*, 2001, **2**, 39-44.

51. T. Kamei, H. Akiyama, H. Morii, N. Tamaoki and T. Q. Uyeda, *Nucleosides Nucleotides Nucleic Acids*, 2009, **28**, 12-28.

52. H. Asanuma, T. Yoshida, T. Ito and M. Komiyama, *Tetrahedron Lett.*, 1999, **40**, 7995-7998.

53. J. P. May, L. J. Brown, I. Rudloff and T. Brown, *Chem. Commun.*, 2003, 970-971.

54. S. A. Marras, F. R. Kramer and S. Tyagi, *Nucleic Acids Res.*, 2002, **30**, e122.

55. M. R. Banghart, A. Mourot, D. L. Fortin, J. Z. Yao, R. H. Kramer and D. Trauner, *Angew. Chem., In. Ed.*, 2009, **48**, 9097-9101.

56. M. K. Beissenhirtz, R. Elnathan, Y. Weizmann and I. Willner, *Small*, 2007, **3**, 375-379.

57. X. Liang, H. Asanuma, H. Kashida, A. Takasu, T. Sakamoto, G. Kawai and M. Komiyama, *J. Am. Chem. Soc.*, 2003, **125**, 16408-16415.

58. X. Liang, R. Wakuda, K. Fujioka and H. Asanuma, *FEBS J.*, 2010, **277**, 1551-1561.

59. D. Matsunaga, H. Asanuma and M. Komiyama, *J. Am. Chem. Soc.*, 2004, **126**, 11452-11453.

60. T. Gunnlaugsson and J. P. Leonard, *J. Chem. Soc., Perkin Trans. 2*, 2002, 1980-1985.

61. N. DiCesare and J. R. Lakowicz, *Org. Lett.*, 2001, **3**, 3891-3893.

62. M. Kovaliov, M. Segal and B. Fischer, *Tetrahedron*, 2013, **69**, 3698–3705.

63. K. M. Guckian and E. T. Kool, *Angew. Chem., Int. Ed.*, 1997, **36**, 2825-2828.

64. D. Young, P. Tollin and H. Wilson, *Acta Crystallogr. Sect. B*, 1969, **25**, 1423-1432.

65. C. Boiziau, B. Larrouy, B. S. Sproat and J. Tolume, *Nucleic Acids Res.*, 1995, **23**, 64-71.

66. H. Inoue, Y. Hayase, A. Imura, S. Iwai, K. Miura and E. Ohtsuka, *Nucleic Acids Res.*, 1987, **15**, 6131-6148.

67. S. M. Freier and K.-H. Altmann, *Nucleic Acids Res.*, 1997, **25**, 4429-4443.

68. L. Stryer and R. P. Haugland, *Proc. Natl. Acad. Sci. U. S. A.*, 1967, **58**, 719-726.

69. A. Sanchez and R. H. De Rossi, *J. Org. Chem.*, 1993, **58**, 2094-2096.

70. A. M. Sanchez, M. Barra and R. H. de Rossi, *J. Org. Chem.*, 1999, **64**, 1604-1609.

71. A. V. Tataurov, Y. You and R. Owczarzy, *Biophys. Chem.*, 2008, **133**, 66-70.